

J.C. Mailhol · P. Ruelle · I. Nemeth

Impact of fertilisation practices on nitrogen leaching under irrigation

Received: 21 March 2000 / Published online: 19 June 2001
© Springer-Verlag 2001

Abstract Field experiments were carried out over a 2-year period on a loamy soil plot under corn in Montpellier (south-east France). The effectiveness of improved irrigation practices in reducing the adverse impact of irrigation on the environment was assessed. Different irrigation and fertiliser treatments were applied to identify the best irrigation and fertilisation strategy for each technique (furrow and sprinkler) to ensure both good yields and lower NO_3^- leaching. No significant differences in corn yield and NO_3^- leaching were found for the climatic scenario of 1999 between sprinkler and furrow irrigation during the irrigation season. Following the rainy events occurring after plant maturity (and the irrigation season), differences in N leaching were observed between the treatments. The study shows that both the fertiliser method, consisting of applying a fertiliser just before ridging the furrows, and the two-dimensional (2D) infiltration process, greatly influence the N distribution in the soil. N distribution seems to have a beneficial impact on both yield and N leaching under heavy irrigation rates during the cropping season. But, under rainy events (particularly those occurring after harvesting), the N, stored in the upper part of the ridge and not previously taken up by plants, can be released into the deeper soil layers in a furrow-irrigated plot. In contrast, the 1D infiltration process occurring during sprinkler irrigation events affects the entire soil surface in the same way. As a result the same irrigation rate would probably increase N leaching under sprinkler irrigation to a greater extent than under furrow-irrigation during an irrigation period. In order to assess the robustness of these interpretations derived from soil N-profile analysis, a modelling approach was used to test the irrigation and fertilisation strategies under heavy irrigation rates such as those occurring at the downstream part of closed-end furrows. The RAIEOPT and

STICS models were used to simulate water application depths, crop yield and NO_3^- leaching on three measurement sites located along the central furrow of each treatment. The use of a 2D water- and solute-transport model such as HYDRUS-2D enabled us to strengthen the conclusions derived from the observations made on the N distribution under a cross-section of furrow. This model helped to illustrate the risk of over-estimation of N leaching when using a simplified 1D solute-transport model such as STICS.

Introduction

Despite certain modernisation efforts, furrow irrigation is still regarded as being wasteful and inefficient. In addition, high irrigation rates coupled with substantial field N fertilisation in some countries (Fernandez et al. 1994) inevitably leads to an increase in the risk of groundwater pollution.

Nevertheless, the specific effect of the two-dimensional (2D)-infiltration process in furrow irrigation on the distribution of N deserves to be analysed in much greater detail. The fact that substantial yields can be obtained, despite moderate fertiliser application (DDAF et al. 1989), means that N-distribution processes under furrow and sprinkler irrigation are significantly different. So, field experiments were carried out to observe N transport under furrow-irrigation conditions and to analyse the impact of a high water application depth (WAD) on NO_3^- leaching and crop yield.

Modelling can be an interesting approach when trying to identify irrigation and fertilisation practices conducive to sustainable agriculture. The STICS (Simulateur mulTIidisciplinaire pour les Cultures Standard) model (Brisson et al. 1998) simulates, at a daily time step, the impact of agricultural practices on yield and NO_3^- leaching during a cropping season (and on the inter-cropping season). It can be considered as an efficient tool when investigating sprinkler-irrigation

practices. But, the applicability of this conceptual model to furrow irrigation is questionable.

Field experiments enable us to determine the initial conditions for water and solutes which include input data for the HYDRUS-2D model (Simunek et al. 1996) which simulates water flow and N transport using the Galerkin finite elements method. Unlike STICS, this model cannot be used to simulate the impact of irrigation and fertilisation practices on NO_3^- leaching and yield at the growing-season scale. But the simulation results of HYDRUS-2D can be used to correct for the soil N profile data of STICS, in particular after a high WAD. It also can be used to give us the magnitude of error for N distribution after irrigation, which is incurred when a 2D infiltration process is assimilated into a 1D infiltration process.

Materials and methods

The experimental site

The experimental plot was located at the Cemagref Institute in Montpellier (42.5°N, 85°W) on a loamy (49%) sandy (30%) clay (21%) soil. In 1999 the experiments consisted of three treatments: two furrow irrigated (Te, Ta), and one sprinkler irrigated (Sp) one. Te and Ta were furrow irrigated over a 130-m length with corn (Samasara variety) sown on 26 May in rows 0.8 m apart. Each of these treatments were composed of around 35 furrows. The whole of the furrow-irrigated plot was laser levelled in February giving a slope of 0.25%. The Sp treatment was installed on a flat plot 30 m in length and 90 m in width. Ridge-furrow tillage was used with a spacing between ridges of 0.8 m and a mean value of 0.16 m for the difference in elevation between the furrow bottom and the ridge top.

A first fertilisation (90 kg N/ha) was applied 1 day before sowing and a second (70 kg N/ha for Te and 85 kg N/ha for Ta) just before ridging the furrows for the whole of the treatments. A third fertilisation of 40 kg N/ha was applied on Te using ammonia gas added to the water of the second irrigation. The Sp treatment was split into two parts: one part received two fertiliser applications of 75 kg N/ha and the other part (Sp0 N) received no fertiliser to obtain a 0 N reference. Note that 150–200 kg N/ha corresponds to the amount of fertiliser N which is generally supplied to corn in the different regions of France.

For surface irrigation, a gated pipe water supply system was used. At the pipe entrance, a tank of 1 m³ ensured a constant hydraulic head and discharges (close to 20 L/s; where L = liter).

In order to insure a homogeneous crop emergence, a low WAD of 28 mm was applied to the whole of the field by using a travelling gun system. The surface-irrigated plots were watered only 3 times owing to some rainfall events (114 mm of rain from June to the end of September). A few days after furrow ridging, Te received 251 mm [averaged inlet discharge (Q_{in}) = 1.18 L/s, cut-off time (t_{co}) = 370 min] for the first irrigation (8 July), 130 mm (averaged Q_{in} = 0.76 L/s, t_{co} = 300 min) for the second (24 July) and 100 mm (Q_{in} = 1.08 L/s, t_{co} = 160 min) for the third irrigation (24 August). Ta received 76 mm (averaged Q_{in} = 1.2 L/s, t_{co} = 110 min) for the first irrigation (8 July), 67 mm (averaged Q_{in} = 0.73 L/s, t_{co} = 160 min) for the second (25 July) and 53 mm (Q_{in} = 0.77 L/s; t_{co} = 120 min) for the third irrigation (25 August). Generally, the water distribution was cut off when the water front of all the furrows in a treatment had reached the end of the plot. The presence of cracks due to a higher clay ratio (25% in Te in relation to 18% in Ta) explains the slower advance of water in Te than in Ta. As a result, the WADs are greater on Te than on Ta.

This irrigation technique was a closed-end furrow method. In contrast, the Sp treatment was fully irrigated (8 times; total WAD = 271 mm) in order to match the estimated maximal

evapotranspiration. In 1998, the experiment was carried out on corn with sprinkler irrigation on the entire experimental plot with calibration of the STICS model being the main objective.

Field data acquisition equipment

Initial N was profiled before sowing at the future measurement sites. Soil samples were collected at 0–30, 30–60, 60–90, 90–120, 120–150 cm depths. During an irrigation event the inlet discharge of each furrow was measured using a portable flume and the advance front of the irrigated furrows was monitored for the stations $x = 20, 30, 50, 70, 90, 110, 130$ m. Three measurement sites for water and N transfers were located on both treatments Ta and Te at upstream ($x = 30$ m), central ($x = 65$ m), and downstream sites ($x = 115$ m) along the central furrow of each treatment.

A series of mercury tensiometers (at 10, 20, 30, 45, 60, 75, 130, 150 cm soil depth) capable of measuring pressure heads between 0 and –80 kPa, and neutron access tubes of 2.5 m in depth, were used. The N concentration in the soil solution was measured by means of a ceramic cup extraction system located at 1.4 m depth. The equipment was installed on the ridge top. A second neutron access tube was placed in the bottom of the furrow.

The monitoring of the infiltration profile was made possible with a series of 30-cm-long CS6115 Campbell time domain reflectometry probes inserted into the soil at four different depths (30, 60, 90, 120 cm soil depth) on the central site of Ta. The probes were placed apart along the furrow to avoid interference with vertical water and solute transfer. At $t = t_{co}$, water heights were measured in the furrows at the downstream end. Water heights varied from 10 to 15 cm depending on the advance time and the cross-section shape for a given furrow. On the Sp treatment site, the amount of water applied was measured using four pluviometers.

In order to establish a N profile in the vertical of the furrow bottom and in the vertical of the ridge top, soil samples were collected from the different treatments. Soil samples were collected from the central and downstream sites before the second irrigation (58 days after sowing), 14 days after (3 August) for the whole of sites, on 9 November for upstream and downstream sites of Te and Ta, on 6 August for all the sites, on 15 October for the mid-site only, and on 9 November for all the sites (October measurements were stopped due to rainfall).

Just before harvesting, seven plant samples per site were collected on 3.6 m² for dry matter and grain yield evaluation.

Analysis of N profiles

The spatial distribution of the N concentration in the furrow cross-section is shown on Figs. 1 and 2. The distribution of N resulted from the ridge-furrow tillage operation which displaced a part of the N which was located in the furrow before ridging, to the ridge top. The choice of the units (kg/ha) and the thickness of the layers

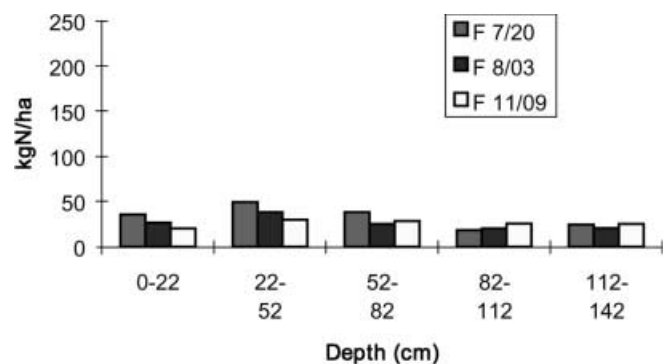


Fig. 1 Evolution of the N profile under the furrow (F) on the downstream site of the furrow-irrigated treatment, Te

emphasise the impact of furrow ridging on the spatial distribution of the N fertiliser. The substantial rainfall recorded after 15 October was responsible for the transfer of N which was then concentrated in the upper part of the ridge. Comparison of Fig. 3 and 4 shows that the entire profile became homogeneous under rainfall. Note that the reference depth (the soil surface) is not the same in the furrow and on the top ridge. The thickness of the first layer is only 22 cm under the furrow bed because 8 cm of soil was removed during ridging; as a result there is one more layer (0–8 cm) on the top ridge. Figure 4 shows that the decrease in the N concentration in the entire profile after 15 October was due to N leaching.

The storage of N in the upper part of the top ridge, during furrow ridging, reduces significantly the risks of NO_3^- leaching during the crop cycle when high irrigation levels are applied. Nevertheless, this N reservoir, which is not consumed by the plant, can be lost after heavy rainfall events at the end of the crop cycle as shown by Figs. 2 and 4. One can therefore assume that under sprinkler irrigation the entire soil profile suffers from leaching, whereas under furrow irrigation runoff reduces infiltration, which in turn limits NO_3^- leaching in the furrow bed during storm events. With precipitation events the N reservoir located in the upper part of the top ridge can release N into the lower part of the top ridge. With respect to this last point, we noticed that N concentration decreases with depth under the furrow (Fig. 1) in contrast with that of the top ridge which increases a little, as shown in Fig. 2. We also can observe that the increase was greater in the 8- to 38-cm soil bracket than in the 0- to 8-cm soil bracket. One can offer two explanations for this phenomenon. First the fertilised irrigation, applied on 22 July, induced a concentration increase under the top ridge and secondly, the rainfalls (50 mm between 28 July and 6 August) probably released a part of the N load from the first layer

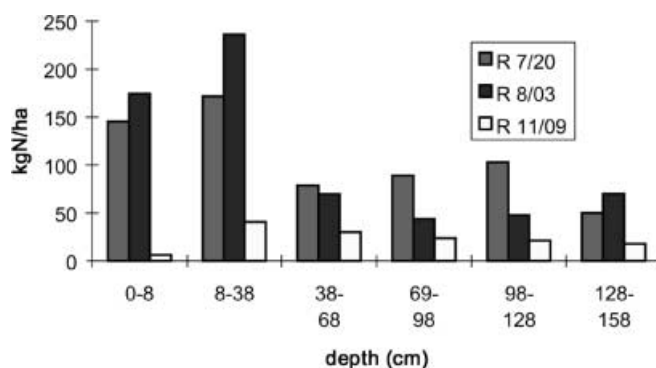


Fig. 2 Evolution of the N profile under the ridge (R) on the downstream site of Te

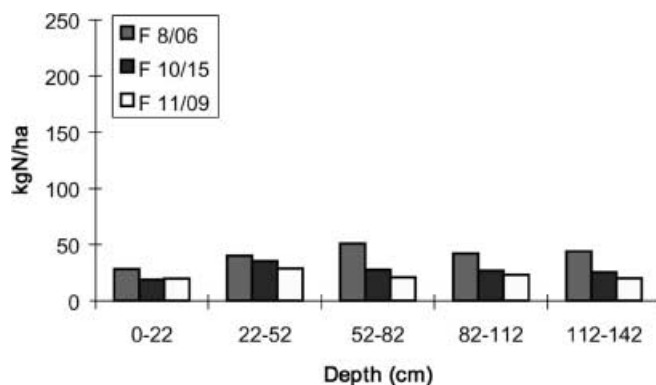


Fig. 3 Evolution of the N profile under the F on the central site of the furrow-irrigated treatment, Ta

to the lower soil layer of the top ridge as confirmed using a 2D modelling approach.

The comparison between the Sp data of Fig. 5 with those of Fig. 3 shows that for the first 10 days of August, the N concentration was lower under the first 30 cm beneath the furrow than in the first 30 cm of the Sp treatment. The opposite was true regarding the subsequent layer. This seems to confirm that N leached from the first to the subsequent layer under the furrow bed. The initial N concentration (25 May) in the deepest layers was greater in Sp (27 kg/ha) than in Ta (11 kg/ha). This explains the lower N concentrations under the top ridge than under Sp irrigation on 9 November. The comparable values which can be observed between the furrow-irrigated treatments (Fig. 3) and Sp (Fig. 5) on November were probably due to N leaching.

Lastly, one can also see that the N concentration fluctuated much more under furrow irrigation than under sprinkler irrigation in the different soil layers in our experimental conditions.

N leaching measurements

N in the soil solution was only measured for the furrow-irrigation treatments. But tensiometer and neutron-probe measurements showed that no drainage (and as a result no NO_3^- leaching) occurred in the Sp treatment during the irrigation season.

N concentrations in the soil solution (mg/l) measured before the rainfall events of September were low for the different sites and treatments. Over the same period, the greatest N concentrations (15 mg/l) were observed in the Te treatment which received much more water and an extra 40 kg N/ha in comparison with Ta. In Ta, the N concentration never exceeded 9 mg/l, even in the downstream

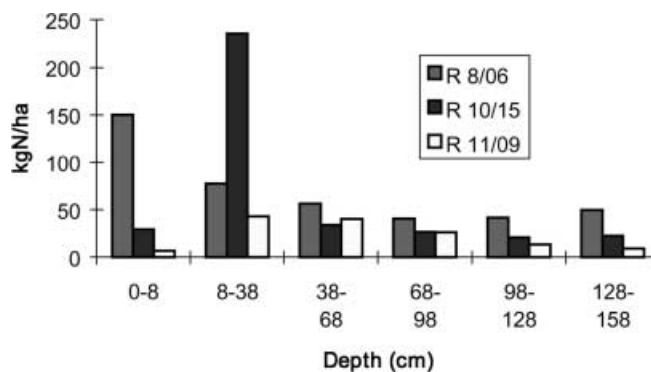


Fig. 4 Evolution of the N profile under the R on the central site of Ta

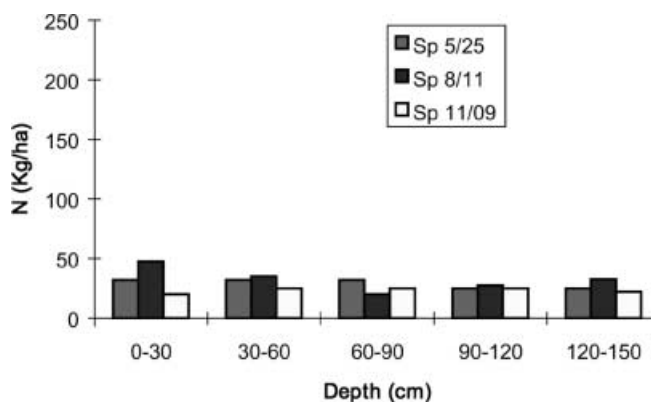


Fig. 5 Evolution of the N profile in the sprinkler-irrigated (Sp) treatment

part of the treatment. Under the rain events of September and October, the greatest values were observed for the downstream part of Te (48 mg/l), whereas for Ta the N concentrations remained under 8 mg/l. In Ta, no drainage was observed until October. The drainage value estimated from the water balance of Ta was 90 mm during the rainy events of October, which gives 7.2 kg/ha leached N, assuming a N concentration of 8 mg/l. Owing to a substantial WAD at each irrigation on the downstream site of Te (cumulative WAD=474 mm), drainage was observed during the irrigation period. The estimated level of leached N in Te from sowing to the end of October was 68 kg/ha. The lack of measurements at the end of October prevented us from estimating the amount of N leached after harvesting. This low value is compatible with the N profile measured on 15 October and shows that some N still remained in the soil between 0 and 1.5 m depth.

WAD estimations

WADs are estimated using the RAIEOPT model (Mailhol and Gonzalez 1993) which was modified for the closed-end furrow technique (Mailhol et al. 1997). Under our loamy soil conditions the advance trajectory (exact solution of the Lewis and Milne equation) is better calibrated using the model derived from Horton infiltration rather than the one derived from linear infiltration: $Z = B + Cst$. These two infiltration equations result from the Parlange equation (Parlange et al. 1982) in its asymptotic form where C_s is assimilated into K_s and $B = S^2/2K_s$, where S is sorptivity and K_s is saturated conductivity. Using the White and Sully approach (1987) and the $K(h)$ Gardner (1958) equation, the Horton equation becomes:

$$Z(\tau) = 0.9\lambda c \times \Delta\theta \times [1 - \exp(-\chi\tau)] + K_s \times \tau \quad (1)$$

where λc is capillary length, $\Delta\theta = \theta_s - \theta_i$, where θ_s is saturated volumetric water content, and θ_i is initial volumetric water content, χ is a calibration parameter and τ is opportunity time. Note that 0.9 is replaced by 1 in the Green-Ampt estimation of S . Table 1 presents the calibration results of the RAIEOPT model. Optimal calibrations are obtained when the χ parameter (having little sensitivity) is given as 0.15/min (averaged value resulting from calibration) for all the irrigation tests.

Furthermore for the first irrigation, the averaged value of capillary length derived from advance calibration is close to that obtained by Revol et al. (1996) on the same plot using the disc

Table 1 Calibration results regarding the two infiltration parameters of the RAIEOPT model [$B = 0.9 \times Ec \times \lambda c \times \Delta\theta$ (where Ec is inter-furrow spacing, λc is capillary length) and $\delta\theta = \theta_s - \theta_i$ (where θ_s is saturated volumetric water content, and θ_i is initial volumetric water content)], with the $Ec = 0.8$ m to express B in L/m, where $L =$ liter) for the first, second and third irrigation on the 30 furrows of Ta; χ (a calibration parameter) is set to 0.15/min. Q_m Average inlet discharge, CV coefficient of variation, C_s parameter derived from the calibration of the advance trajectory

First irrigation

$Q_{in} = 1.2$ L/s; $CV = 7\%$
 $B = 24$ L/m ($\lambda c = 20$ cm); $CV = 22\%$
 $C_s = 0.23$ L/m per min; $CV = 20\%$
 $R^2 = 0.9971$; $CV = 0.2\%$

Second irrigation

$Q_{in} = 0.73$ L/s; $CV = 14\%$
 $B = 20$ L/m ($\lambda c = 12$ cm); $CV = 20\%$
 $C_s = 0.160$ L/m per min; $CV = 18\%$
 $R^2 = 0.9886$; $CV = 0.1\%$

Third irrigation

$Q_{in} = 0.77$ L/s; $CV = 4.5\%$
 $B = 15$ L/m ($\lambda c = 10$ cm); $CV = 19\%$
 $C_s = 0.160$ L/m per min; $CV = 17\%$
 $R^2 = 0.9873$; $CV = 0.3\%$

permeameter (Perroux and White 1988), which is associated with the transient flux rate method (Smetten and Clothier 1989). As we shall see later, the parameter C_s derived from calibration of the advance trajectory, is within the order of magnitude (using an inter-furrow spacing of 0.8 m to transform L/m to mm) of K_s measured by Revol (1990) on the same plot using the zero plan flux method. So, the possibility of using this model as a predictive approach is underlined by our results. Table 2 shows the WADs simulated for the different sites and opportunity times.

Results

Corn yield results

Average measured grain yields (SD) obtained on Ta were: 12.6 (0.6), 12.7 (0.6) 12.3 (0.8) t/ha for the three sites located at $x = 30$ m, $x = 65$ m and $x = 115$ m, respectively. We are not convinced that the sensitive decrease in yield was due to N leaching, inasmuch as the yield of corn was noticeably higher (with well-developed cobs) at the end of the plot ($125 < x < 130$ m). So we assume that the yield differences between sites were not significant. Averaged grain yield observed for the Sp treatment was 13.8 t/ha with a SD of 1.1 t/ha. It is noticeable that the yield difference is low between the furrow-irrigated treatments and the Sp treatment. Student's t -test shows that the difference is not significant at the 5% level.

Further investigations should be carried out in order to verify if this low yield difference (although it was not significant according to the experimental conditions of 1999) was due to a higher N-use efficiency under sprinklers than under furrow irrigation due to the fact that some fertiliser was stored in the upper part of the ridge during plant growth. As for the fact that corn yield seemed higher on the last 10 m of the furrows, this could result from the high water depths ($12 < h_0 < 15$ cm) in the furrows favouring the transfer of N from the upper part to lower part of the ridge.

The 2D water and solute transport model HYDRUS-2D

The governing flow equation is given by the following modified form of the Richard equation:

$$\frac{\partial\theta}{\partial t} = \frac{\partial}{\partial x_i} \left[K \left(K_{ij}^A \frac{\partial h}{\partial x_j} + K_{iz}^A \right) \right] - S \quad (2)$$

Table 2 Measured water application depths (WAD, mm) and opportunity times (τ , min) for the furrow-irrigated Ta treatment. WAD is calculated in millimetres according to an Ec of 0.8 m

| x (m) | First Irrigation | | Second irrigation | | Third irrigation | |
|---------|------------------|--------|-----------------------|--------|-----------------------|--------|
| | WAD | τ | WAD | τ | WAD | τ |
| 30 | 75 | 105 | 63 | 155 | 43 | 120 |
| 65 | 67 | 120 | 59 (62 ^a) | 170 | 40 (43 ^a) | 110 |
| 115 | 80 | 380 | 91 | 520 | 77 | 480 |

^aobserved WAD using TDR method

where h is the pressure head, S a sink term, x_j ($j=1, 2$) are the spatial coordinates, t is time, K_{ij}^A are components of a dimensionless anisotropy tensor K^A , and K is the unsaturated hydraulic conductivity function given by:

$$K(h, x, z) = K_s(x, z)K_r(h, x, z) \quad (3)$$

The sink term, S , represents the volume of water removed per unit time from a unit volume of soil due to plant water uptake. S is defined according to the Feddes et al. (1978) approach. The Galerkin finite element method with linear basis functions is used to obtain a solution to the flow equation, subject to the imposed initial and boundary conditions.

Initial and boundary conditions

Initial and boundary conditions for the simulation of an irrigation event are presented in Fig. 6. The initialisation of HYDRUS-2D involves h instead of θ . According to the fact that h cannot always be derived from the tensiometers before an irrigation event (particularly when $|h| > 800$ cm), the retention curve (see later) is used to propose h values from the measured $\theta(z)$ profile. Note that for redistribution, initial h conditions are those calculated by the model at the end of the simulated irrigation event; h_0 is given as equal to 0 so the evapotranspiration flux affects both the furrow bed and the ridge.

The governing solute transport equation

The Galerkin finite element method is also used to solve the following solute transport equation subject to appropriated initial and boundary conditions:

$$\frac{\partial \partial c}{\partial t} + \frac{\partial \rho s}{\partial t} = \frac{\partial}{\partial x_i} \left(\theta D_{ij} \frac{\partial c}{\partial x_j} \right) - \frac{\partial q_i c}{\partial x_i} + \mu_w \theta c + \mu_s \rho s + \gamma_w \theta + \gamma_s \rho - S c_s \quad (4)$$

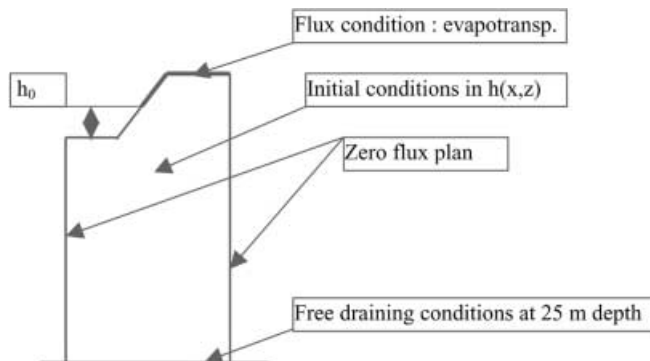


Fig. 6 Schematic representation of the initial and boundary conditions for an irrigation event

where c is the solution concentration, s is the adsorbed solute concentration, q_i is the i th component of the volumetric flux, μ_w and μ_s are first-order rate constants for solutes in the liquid and solid phases, respectively; ρ is the soil bulk density, S is the sink term of the water flow Eq. 2, c_s is the concentration of the sink term, D_{ij} is the dispersion coefficient tensor. The four zero- and first-order rate constants in Eq. 4 may be used to represent a variety of reactions or transformations including biodegradation, volatilisation, precipitation and radioactive decay.

The adsorption isotherm relating s and c is described by the linear equation of the form:

$$s = Kdc \quad (5)$$

where Kd is an empirical constant.

The components of the dispersion tensor, D_{ij} in Eq. 3 are given by:

$$\theta D_{ij} = D_T |q| \delta_{ij} + (D_L - D_T) \frac{q_j q_i}{|q|} + \theta D_m \tau \delta_{ij} \quad (6)$$

where D_m is the molecular diffusion coefficient in free water, τ is a tortuosity factor, $|q|$ is the absolute value of the Darcian fluid flux density, δ_{ij} is the Kronecker delta function ($\delta_{ij}=1$ if $i=j$ and $\delta_{ij}=0$ if $i \neq j$), and D_L and D_T are the longitudinal and transverse dispersivities, respectively.

The water flow parameters

In order to respect the application conditions of the Richard model (the water flux must be Darcian), HYDRUS-2D could only be applied to the Ta treatment where there was no cracking. The parameters α , n and m (with $m = 1 - 1/n$ according to the Mualem model) of the Van Genuchten equation (Van Genuchten 1980) for the retention curve, $h(\theta)$, were calibrated using the measured values of pressure head and soil water content at the same depth, z . The parameter values for the first 16-cm layer were derived from the (h, θ) couple values obtained by Revol (1994) on the same plot using the disc permeameter. For this soil layer, and for the Mualem model, $\alpha = 0.049/\text{cm}$ and $n = 1.292$. The value of θ_s for this soil layer is $0.38 \text{ cm}^3/\text{cm}^3$ and θ_r was set at 0. The value of K_s for the first irrigation is 2.4 cm/h with a bulk density of 1.49 . This K_s value, derived from the zero flux plan method (Vachaud et al. 1978), is related to the first soil layer (0–16 cm), which is ploughed. This value was applied to the upper part of the top ridge and maintained for the entire irrigation season.

The evolution of soil parameters such as K_s and λc (see Table 1) between the first and third irrigation is a well-recognised phenomenon (Berthomé 1991; Or 1996; Mailhol et al. 1999). The soil becomes more and more compact due to the alternation of wetting and drying phases. The slight increase in bulk density from 1.57 after the first irrigation to 1.59 after the second irrigation led to a decrease in K_s from 1.3 to 1.2 cm/h when using the Campbell (1985) model:

$$K_s = 14.4 \left(\frac{1.3}{d_s} \right)^{1.3b} e^{-6.9m_a - 3.7m_i} \quad (7)$$

where m_a and m_i are the clay and loam fraction respectively and b a calibration parameter ($b = 8.4$). But we can consider that this bulk density increase is of little significance in contrast with that occurring after the first irrigation ($1.49 \rightarrow 1.57 \text{ cm}^3/\text{cm}^3$). These last K_s values with $\alpha = 0.017$ and $n = 1.384$ derived from the (h, θ) values measured at the central site of Ta (Fig. 7) are assigned to the entire soil profile under the furrow bed level (16 cm under the top ridge). As a result, two different soil layers are considered in the simulation.

Calibration of the solute transport parameters

The second irrigation was chosen for the calibration of the solute transport parameters of HYDRUS-2D because it occurred between the two N soil sampling dates: 20 July for the first and 3 August for the second. During this 13-day period, soil water redistribution, plant water uptake and N uptake were simulated by the model. Plant water uptake was simulated by the model using the Feddes approach (Feddes et al. 1978) where a root density is assigned to the specified nodes. The sink term of the solute transport equation corresponding to the plant water uptake is set using a N concentration in the transpired water calculated on the basis of plant N requirements. The calibration resulted in the simulation of the measured N profile of 3 August.

Except for the bulk density in the upper part of the ridge, the solute transport parameters were assumed to be constant with soil depth. The molecular diffusion coefficient, D_m , as proposed by Beven et al. (1993) is set equal to $1.55 \text{ cm}^2/\text{h}$. Longitudinal (D_L) and transverse (D_T) dispersivity values are, respectively, initially set equal to 10 cm and 2 cm as used in Simunek et al. (1996) for the furrow example. Results are better when using $D_L = 15 \text{ cm}$ and $D_T = 6 \text{ cm}$. The value of D_L is close to the average dispersivity value proposed by Beven et al. (1993) for a soil similar to that of our plot. A variation of 80% in the previous parameters does not significantly

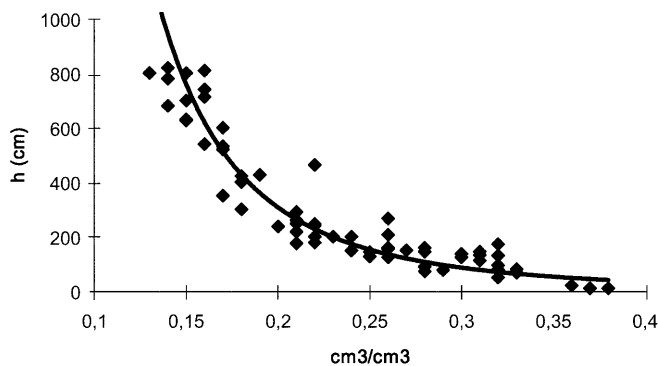


Fig. 7 Retention curve $[h(\theta)]$ for the central site of Ta ($0.15 < z < 1.6 \text{ m}$)

change the simulation results, indicating low sensitivity of the model concerning the dispersivity parameters.

In addition to the soil solute dispersivity, the isotherm partition coefficient, k_d , (L/kg) which linearly relates the solute in the soil solution and in the sorption sites, is required. The k_d constant for NH_4^+ is between 0.3 L/kg and 3 L/kg (Vereecken et al. 1991), whereas that of NO_3^- is very low (10^{-6} L/kg) because it is not adsorbed on the porous matrix. The four zero- and first-order rate constants used in the partial differential equation governing the 2D solute transport during transient water flow are set at zero. This option is justified as the different transformations including biodegradation, volatilisation, etc., can be ignored during this relatively short period. The previous D_L and D_T values with a global (the NO_3^- concentration is at least 5 or 10 times greater than that of NH_4^+) solute distribution constant, k_d , of 7.510^{-4} L/kg permits a satisfactory simulation of N transfer (see Fig. 8a, b) during the second irrigation on the downstream site of Ta assuming the same initial and final N profile as that of Te. One can observe that during N redistribution, the N concentration increases in the upper part of the top ridge as simulated by the model.

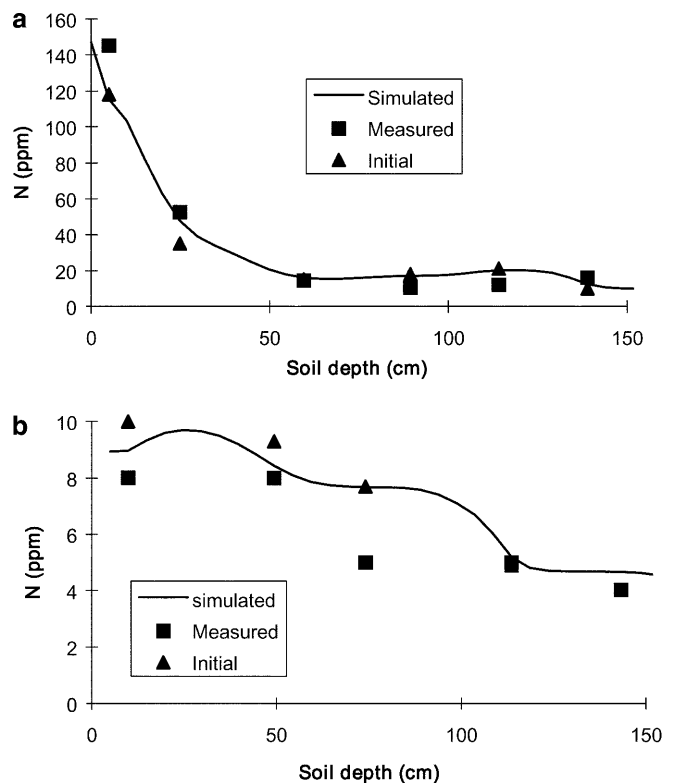


Fig. 8 a N profile under top ridge on 3 August (13 days after the second irrigation) on the downstream site of Ta (initial profile was measured on 20 July; $\tau = 480 \text{ min}$). b N profile under the furrow bed on 3 August (13 days after the second irrigation) on the downstream site of Ta (initial profile was measured on 20 July; $\tau = 480 \text{ min}$)

HYDRUS-2D application

The third of Ta was chosen as an example of a HYDRUS-2D application. Simulation results regarding soil water content at $x=65$ m (central site) and for $x=130$ m (furrow end) are presented in Fig. 9a, b.

At the end of the plot ($x=130$ m), cumulative infiltration simulated on a half furrow gives 520 cm^2 for $\tau=8$ h. This corresponds to 130 mm (inter-furrow spacing = 0.8 m). This value is close to that simulated by the RAIEOPT model, i.e. 125 mm. At the central section of Ta, the simulated cumulative infiltration for $\tau=120$ min, under a surface pressure head of $h_0=5$ cm, equals 39 mm (156 cm^2). It is not significantly different from that simulated by RAIEOPT, i.e. 40 mm.

N distribution after the second and third irrigation was not greatly affected in the vicinity of the top ridge at the central site where $\tau=110$ min ($h_0 \cong 5$ cm), although the model simulates the observed displacement of N due to capillary action in the upper part of the top ridge, which increases the N concentration locally. In contrast, at the ponding part of the furrow end (where $\tau \cong 8$ h, $0 < h_0 < 15$ cm), the N distribution surrounding the top ridge is significantly affected.

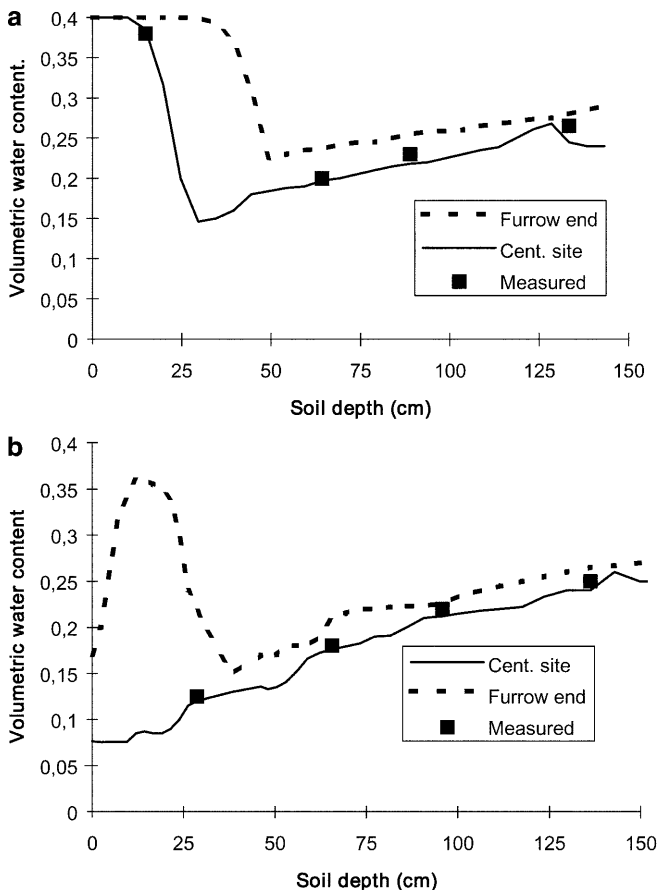


Fig. 9 **a** Soil water content profile under the furrow after the third irrigation of Ta. **b** Soil water content profile under the top ridge after the third irrigation of Ta

A second example of redistribution accounting for plant water and N uptake was simulated for the period between two soil sampling dates (from 26 August to 15 October). The estimated N load due to mineralisation (not simulated by HYDRUS-2D) is derived from that of the Sp0 N treatment. As shown in Fig. 10a, b, HYDRUS-2D simulates the N displacement from the upper part of the top ridge to the deeper soil layers due to rainfall (around 100 mm over the simulated period).

Even with three WAD close to 120 mm at $x \cong 130$ m, no leaching was observed at the end of the plot. In addition, a residual quantity of N, albeit lower than that of central site (owing to a higher h_0 value), was stored at the upper part of the top ridge. The model simulates the release of this residual N to the sub-soil layer under rainfall events occurring from the end of August to mid-October.

Simulations with the STICS model

The STICS model is a crop model which simulates water balance and crop growth for a daily time step for a given water and fertiliser management regime. The water and solute transfer is simulated using the reservoir approach. The soil is divided into discrete layers of 1 cm [according to the Burns (1975) approach regarding solute transfer]. In addition to plant N uptake, only N mineralisation, governed by three pools (humus, crop residue, microbial biomass) is modelled.

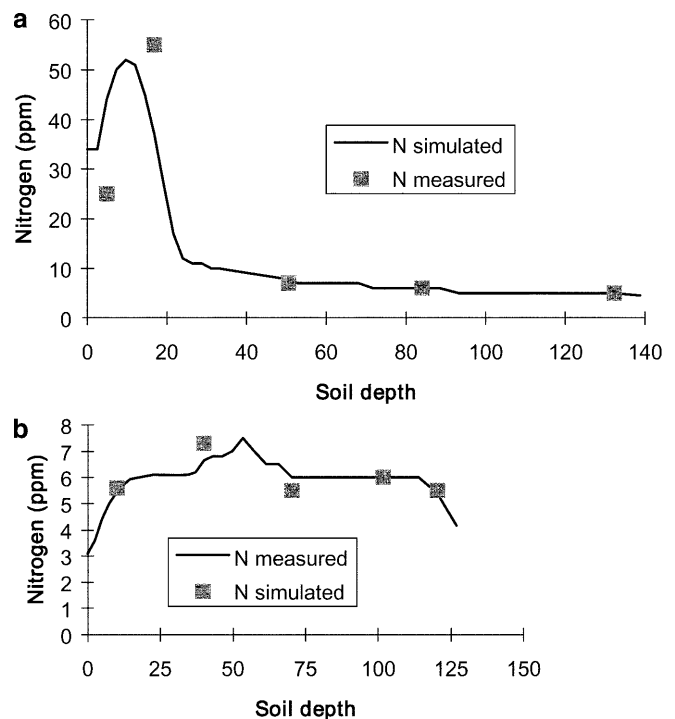


Fig. 10 **a** Test of the two-dimensional (2D) transport model: N profile under the ridge of the central site (On 15 October). **b** Test of the 2D solute transport model: N profile under the furrow on the central site (on 15 October)

The STICS model was calibrated in 1998 on the same plot which was sprinkler irrigated and under corn. For 1999 data, STICS satisfactorily simulated dry matter (22.5 t/ha against the 23 t/ha observed) but underestimated grain yield (12.7 t/ha against the 13.8 t/ha observed) for the fully sprinkler-irrigated treatment. No N leaching was simulated by STICS during the irrigation period. After the last rain events of October, the value simulated by STICS was 23 kg/ha.

Applying STICS to the downstream site of Ta gives 34 kg/ha of leached N against 7.2 kg/ha derived from the ceramic cup measurement and drainage calculation.

The application of STICS to the maximum WAD (WAD = 404 mm at $x = 130$ m) on Ta gives 64 kg/ha of leached N, but without a sensitive impact on the yield due to the fact that N leaching occurred after the crop had matured. The corn yield would have been probably lower at the downstream than at the upstream end if the climatic conditions of summer 1999 had enabled us to apply three or four additional water applications as is usually the case in southern France.

For an average climatic scenario, such as that of 1998, for the maximum WAD on Ta, STICS gave a simulated value of 67 kg/ha leached N at the end of the irrigation season, which required six water applications (WAD = 650 mm at $x = 130$ m) to avoid water-stress conditions in the upstream part of the plot. The simulated yield was significantly decreased, i.e. 10.4 t/ha compared to 13 t/ha observed on the fully sprinkler-irrigated treatment (WAD = 350 mm for the MET treatment).

Discussion

Analysis of N soil profiles under the furrow bed and under the ridge over the cropping season show that N accumulation on the top ridge, due to the ridging operation, was only marginally affected by 2D water transfer. At the end of the irrigation season, furrow and ridge N profiles continued to contrast greatly. Over the rainy events of October 1999, the differences between the two N soil profiles were considerably reduced. In contrast with furrow irrigation, sprinkler irrigation results in much lower fluctuations of N concentration in the different soil layers.

Using field observations and 2D-model simulations one can deduce that N leaching is not significant and, as a result, yield levels are not as affected under high rates of furrow irrigation as could be expected. The application of HYDRUS-2D confirms the weak contribution of the N located on the upper part of top ridges to the N-leaching process. The split application of N fertiliser: the first application 90 kg N/ha, given just before sowing (in the case of a late sowing date due to a rainy spring) the second one 70 kg N/ha applied just before ridging furrow, seems to reduce the risk of N leaching (during the crop cycle) and consequently the possibility of a lower yield is also decreased. Nevertheless, the fraction of N stored in the upper part of top ridges and not consumed

by the plant may leach to the subsoil under post-harvest precipitation.

This study shows that the use of a crop model such as STICS, which does not account for the 2D solute-transfer process, can over-estimate N leaching during the crop cycle and under-estimate the yields on furrow-irrigated plots. In addition, NO_3^- leaching during the inter-cropping season can be under-estimated.

Combining the RAIEOPT and STICS models could be considered as an effective approach when predicting the impact of irrigation on yield and drainage under no N-uptake limitation. These two models can be effectively calibrated and used with field data. Nevertheless, investigations still have to be carried out to check if the reliability of the simulation can be improved by using an adequate weighting factor which would allow the N distribution within the soil to be predicted.

References

- Berthomé P (1991) Modélisation de l'infiltration en irrigation à la raie: résolutions numérique et analytique. Application à l'étude de la conduite des arrosages. PhD thesis. Institute Polytechnique de Toulouse, Toulouse
- Beven KJ, Henderson D, Reeves AD (1993) Dispersion parameters for undisturbed partially saturated soil. *J Hydrol* 143:19–43
- Brisson N, Mary B, Ripoche D, Jeufroy MH, Ruget F, Nicoulaud B, Gate P, Devienne-Barret F, Antonioletti R, Durr C, Richard G, Beaudoin N, Recous S, Tayot X, Plenet D, Cellier P, Machet JM, Meynard JM, Delécolle R (1998) STICS: a generic model for the simulation of crops and their water and nitrogen balances. I. Theory and parametrisation applied to wheat and corn. *Agronomie* 18:311–346
- Burns IG (1975) An equation to predict the leaching of surface-applied nitrate. *J Agric Sci* 85:443–454
- Campbell GS (1985) Soil physics with BASIC. Transport models for soil-plant systems. Elsevier, Amsterdam
- DDAF Arles, Cemagref, SCP, ARDEPI (1989) Acquisition de références technico-économiques sur les matériels d'irrigation de surface (ARTHEMIS). DDAF Arles, Cemagref, SCP, ARDEPI, Groupement d'Aix en Provence, Aix en Provence
- Feddes RA, Kowalik PJ, Zaradny H (1978) Simulation of field water use and crop yield, simulation monographs. Pudoc, Wageningen, The Netherlands
- Fernandez JE, Moreno F, Cabrera JM, Murillo E, Fernandez-Boy (1994) In: Water and nitrogen use efficiency in a maize crop in southern Spain. International Conference on Land and Water Resource Management in the Mediterranean Region, vol I. Institute Mediterranean, Bari, Italy
- Gardner WR (1958) Some steady state solutions of the unsaturated moisture flow equation. *Soil Sci* 85:228–232
- Mailhol JC, Gonzalez G (1993) Furrow irrigation model for real-time applications on cracking soils. *ASCE J Irrig Drain Eng* 119(5):768–783
- Mailhol JC, Baqri H, Lachhab M (1997) Operative irrigation furrow modelling for real-time applications on closed-end furrows. *Irrig Drain Syst* 11:347–366
- Mailhol JC, Priol M, Benali M (1999) A furrow irrigation model to improve irrigation practices in the Gharb valley of Morocco. *Agric Water Manage* 42:65–80
- Or D (1996) Wetting-induced soil structure changes. The theory of liquid phase sintering. *Water Resour Res* 2(10):3041–3049
- Parlange JY, Lisle I, Braddock RD (1982) The three parameters infiltration equation. *Soil Sci Soc Am J* 133(6):337–341
- Perroux HL, White I (1988) Design for disc permeameter. *Soil Sci Soc Am J* 52:1205–1215

- Revol P (1990) Modélisation simplifiée de l'infiltration appliquée à la micro-irrigation. Mémoire de DEA. University Joseph Fourier, Grenoble, France
- Revol P (1994) Caractérisation hydrodynamique des sols par infiltration axisymétrique et modélisation simplifiée de la micro-irrigation. PhD thesis. Université Joseph Fourier, Grenoble I
- Revol P, Clothier BE, Mailhol JC, Vachaud G, Vauclin M (1996) Infiltration from a surface point source and drip irrigation. 2. An approximation time-dependant solution for wet-front position. *Water Resour Res* 33(8):189–1874
- Simunek J, Sejna M, Van Genuchten MT (1996) HYDRUS-2D. IGWMC, USDA/ARS Riverside, Calif.
- Smetten KRJ, Clothier B (1989) Measuring unsaturated sorptivity and conductivity using multiple disc permeameters. *J Soil Sci* 40:563–568
- Vachaud G, Dancette C, Sonko, Thony JL (1978) Méthodes de caractérisation hydrodynamique in situ d'un sol non saturé. Application à deux types de sol du Sénégal en vue de la détermination des termes du bilan hydrique. *Soil Sci Soc Am J* 44:892–898
- Van Genuchten MT (1980) A close-form equation for predicting the hydraulic conductivity of unsaturated soils. *Soil Sci Soc Am J* 44:892–898
- Vereecken H, Vanclooster M, Swerts M, Diels J (1991) Simulating water and nitrogen behavior in soil cropped with wheat. *Fertil Res* 27:233–243
- White I, Sully J (1987) Macroscopic and microscopic capillarity length and time scales from field infiltration. *Water Resour Res* 23:1514–1522